Crack Opening Displacement Measurement Methods for Crack Arrest Experiments

J. H. GIOVANOLA and T. KOBAYASHI
Metallurgy and Fracture Mechanics Program, SRI International, Menlo Park, CA 94025, USA

ABSTRACT

We present two methods for measuring the crack opening displacement (COD) in crack arrest experiments. One method relies on remote dynamic crack face opening displacement measurements, whereas the other is based on posttest fractographic reconstruction of the crack tip deformation. COD measurements were performed using the two techniques for cleavage crack arrest experiments simulating pressurized thermal shock conditions in A533B pressure vessel steel. The COD values measured by the two methods agreed well, and a good correlation was found between the COD history and the fracture events. From these results we conclude that (1) dynamic crack face profiles can readily be measured in crack arrest experiments, and these data can then serve to verify numerical simulations of the crack arrest experiment; (2) estimates of the COD can be obtained from remote displacement measurements; and (3) fractographic COD measurements can help evaluate the influence of specimen size thickness and triaxial constraint on the arrest toughness.

KEYWORDS

Crack opening displacement; crack opening angle; cleavage crack extension; arrest toughness; dynamic displacement measurement; topographic analysis of fracture surfaces; A533B steel.

INTRODUCTION

In recent years, many experiments have been performed to establish the cleavage crack arrest capabilities of nuclear pressure vessel steels. Small transverse wedge-loaded compact tension specimens, wide plate (deWit and Fields, 1988), and thick, axially cracked cylinders (Bryan et al., 1986) have been used in these investigations. The arrest toughness has been characterized almost exclusively in terms of the stress intensity factor of linear elastic fracture mechanics. Most crack arrest tests are evaluated by calculating the stress intensity factor at arrest using either dynamic numerical simulations of the experiments or a quasistatic approximation to obtain the stress intensity factor at arrest from known static solutions.

Several factors limit the reliability of these crack arrest evaluation methods. First, uncertainty about the experimental boundary conditions (for example, in wide plate experiments) often limits the reliability of numerical simulations to calculate the stress intensity factor. Second, the influence on crack arrest toughness values of the specimen size, geometry, and thickness is not fully understood, so that comparison of results from different test configurations is difficult. Third, characterization of the arrest toughness in terms of the stress intensity factor neglects plastic and viscoplastic effects, which may be significant, particularly in small specimens.

These problems can be addressed by performing crack face opening displacement measurements to verify computed displacements and validate boundary conditions used in the simulations. In addition, since the COD is a local parameter independent of any constitutive assumption, COD measurements may serve as an alternative parameter for characterizing dynamic crack propagation and arrest events and for verifying arrest toughness results. We present and compare two promising techniques for obtaining crack opening displacement data from dynamic fracture experiments. Measurements for cleavage crack arrest experiments in A533B Class 1 pressure vessel steel are discussed to illustrate the potential of the two techniques. More details about the investigation are given in Kobayashi and Giovanola (1988).

COD MEASUREMENT TECHNIQUES

We refer to the crack opening displacement (COD) as the displacement of the crack faces at a fixed distance behind the crack tip. The associated concept of crack opening angle (COA) is then defined as the ratio of the crack opening displacement and the distance from the crack tip.

Our first measurement technique derives the COD from global specimen displacement measurements. We measured the crack face opening profile with custom-built displacement transducers (Hall effect displacement transducers, HEDITs) and combined these data with the crack extension history to reconstruct the near crack tip profile. The HEDIT measures the relative displacement of a Hall effect sensor with respect to a permanent magnet by converting changes in the magnetic field strength as of function of position into an electrical output (Giovanola et al., 1988). To measure crack face opening displacement histories during dynamic crack propagation and arrest experiments, the HEDIT is mounted on the side surface of the specimen across the crack line, with the Hall effect sensor and the magnet each fastened to one of the opposite crack faces.

Our second measurement technique derives the COD directly from measurements of the local deformation at the crack tip using an advanced posttest fractographic method, fracture surface topography analysis (FRASTA). FRASTA uses a computer technique to compare quantitative three-dimensional topographs of conjugate fracture surfaces (matching fracture surfaces from each half of a broken specimen or part) and to reconstruct the details of the fracture process. A more detailed description of the technique is given in Kobayashi and Shockey (1987). A significant advantage of FRASTA is that it can reconstruct postmortem the crack opening profile for speciemens tested under dynamic loading conditions.

CRACK ARREST TESTS

The COD measurements described in this paper were performed on so-called moment-modified compact tension (MMCT) specimens, designed by Ayres and coworkers to simulate cleavage crack propagation and arrest under pressurized thermal shock conditions (Ayres et al., 1988). The MMCT specimen and its main planar dimensions are shown schematically in Figure 1. The specimen consists of a transversely wedge-loaded compact tension specimen, to which two large pull tabs have been added. The tensile load applied by the pull tabs simulates pressure-induced loads and produces a static stress intensity, which increases with crack length. The load applied by the wedge at the starter fatigue precrack simulates the effect of the thermal stresses and is used to initiate a running crack. An increasing fracture toughness field along the crack path is achieved by imposing a linear temperature gradient over the specimen length (-40°C at the initial crack tip, 100°C at the opposing edge).

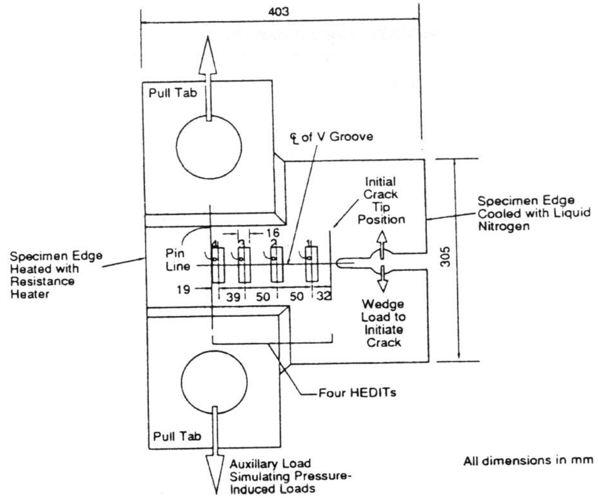

Fig. 1. Moment-modified compact tension specimen and position of HEDITs along crack path.

We measured dynamic crack face opening displacements using HEDITs during one MMCT experiment (MMCT9). Four HEDITs were mounted on the specimen at the locations indicated in Figure 1. During this experiment, the crack velocity was also measured using strain gages along the crack path. The initial crack velocity was over 900 m/s.

The FRASTA measurements were performed on another specimen fractured in a test (test MMCT7), which was an exact duplicate of test MMCT9. Fractographic evidence shows that in tests MMCT7 and MMCT9, the crack propagated in cleavage for about 170-190 mm, arrested at a location where the temperature was 36° to 38°C, then reinitiated, again in cleavage, and finally arrested after approximately 20-30 mm of additional extension.

RESULTS

HEDIT Measurement Results

The crack face opening displacement histories measured with four HEDITs during tests MMCT9 are shown in Figure 2, together with the times of the first crack arrest (480 μs), reinitiation (990 μs), and second crack arrest (1060 μs). Note that all the displacements continue to increase monotonically after the first crack arrest. Figure 3 shows plots of the crack face opening profiles constructed as a function of selected times from the data in Figure 2. Figure 3(a) shows the overall crack opening profile during the entire experiment. Figure 3(a) indicates that during most of the crack extension the crack profile remains sharp. Moreover, a more detailed analysis of the profiles reconstructed from the HEDIT measurements suggests that during the last 30 mm of extension the near tip opening angle increases rapidly, suggesting in turn that the resistance to crack extension also rises. This point is illustrated in Figure 3(b), which is a time sequence of estimates of the near crack tip profile during the arrest phase. To construct Figure 3(b), the remote crack face opening profiles for the times of interest were constructed from the HEDIT 3 and 4 displacement values. The corresponding crack tip position was estimated from the crack extension history, and approximate near tip opening profiles were drawn by connecting the crack tip location with the point representing the remote opening profile 1.5 mm behind the crack tip.

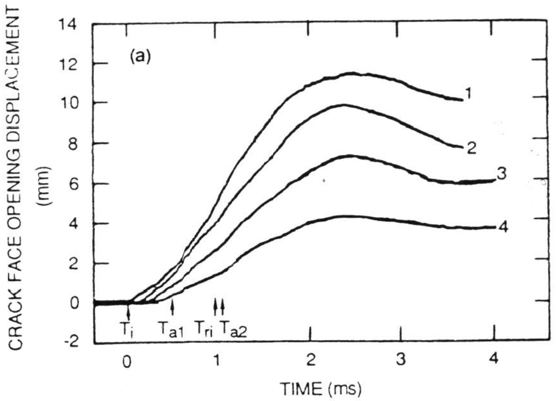

Fig. 2. Crack face opening displacement histories in specimen MMCT9 (T_i = time of crack initiation from fatigue precrack tip, T_{a1}= 480 μs, time of first crack arrest, T_{ri} = 990 μs, time of crack reinitiation, T_{a2} = 1060 μs, second and permanent crack arrest.)

Table 1 lists the values of the crack opening displacement measured 1.5 mm behind the crack tip in Figure 3(a) for times between arrest and reinitiation. Columns at left present the data obtained for the average position of the crack tip; columns at right present the data obtained for the leading part of the crack front, assuming that it precedes the average crack position by 9 mm, as observed on the fracture surface. The data in Table 1 indicate that significant blunting of the crack tip occurs after arrest.

Table 1. Summary of HEDIT results for specimens MMCT9

	Average Crack Front		Leading Edge of Crack Front	
Time (μs)	COD, 1.5 mm Behind Crack Tip (μm)	COA (radians)	COD, 1.5 mm Behind Crack Tip (μm)	COA (radians)
300	130	0.087	90	0.060
380	190	0.127	90	0.060
430	240	0.160	140	0.093
480 (arrest)	320	0.213	210	0.140
600	480	---	340	---
700	640	---	440	---
800	800	---	580	---
900	970	---	740	---
990 (reinitiation)	1140	---	860	---

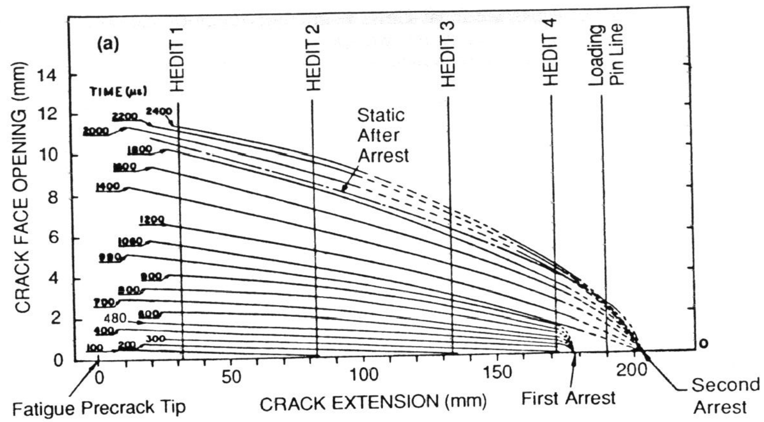

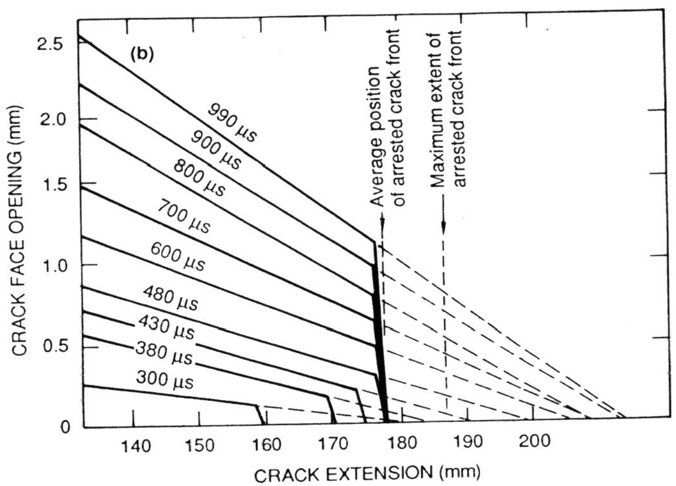

Fig. 3. Crack face opening profiles at various times during experiment MMCT9. (a) Overall crack profiles (b) estimate of near crack tip profiles.

FRASTA Results

We present the results of the FRASTA analysis in the first crack arrest region of test MMCT7. Both crack extension and the crack opening profiles are reconstructed by the FRASTA analysis and are displayed here in the form of cross-sectional plots, with the cross-sectional plane perpendicular to the crack plane and to the crack front.

Figure 4 shows a series of cross-sectional views at the midsection of specimen MMCT7 for increasing separation distance between the two specimen halves. The midsection position corresponds to the position of maximum crack front extension. Figures 4(a) and 4(b) illustrate the last part of the crack propagation phase. Figure 4(c) shows the crack face profile immediately after arrest. Figures 4(a) through 4(c) indicate that the crack maintains a sharp tip up to the point of arrest, but that although the crack tip remains sharp, the COD and COA increase significantly during the last millimeter of extension. Figure 4(d) shows blunting of the crack shortly after arrest, and Figure 4(e) shows the blunted crack just before reinitiation.

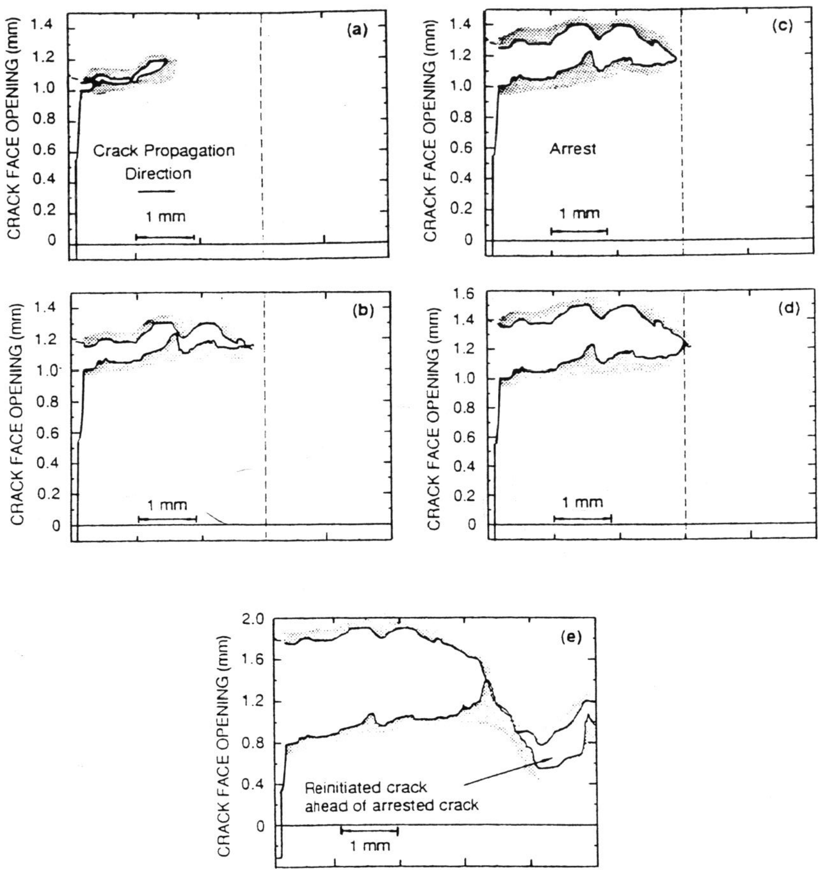

Fig. 4. Near tip crack opening profiles for specimen MMCT7 reconstructed with FRASTA. (a) and (b) last increments of crack extension, (c) immediately after arrest, (d) crack blunting after arrest, (e) just before complete reinitiation.

Table 2. Summary of FRASTA results for specimen MMCT7

Crack Tip Position Relative to Arrested Crack Tip Position (mm)	COD (μm)	COA (radians)
- 1.6	40	0.027
- 0.2	140	0.093
Arrest	220	0.147
Blunting	340	---
Reinitiation	850	---

Values of the COD 1.5 mm behind the crack tip (and when appropriate of the COA) obtained from the FRASTA reconstruction are listed in Table 2. The arrested crack blunts significantly up to the point of the second reinitiation. This observation is consistent with the behavior deduced from HEDIT measurements.

DISCUSSION

The remote crack face opening displacement measurements performed during test MMCT9 demonstrate that with appropriate transducers crack face opening profiles can be readily obtained during crack propagation and arrest experiments and that valuable information about the influence of specimen dynamics on the fracture events can be obtained from such measurements. In particular, as suggested in the Introduction, measured crack opening profiles can be compared to profiles calculated in numerical simulations to verify the numerical results and the assumed boundary conditions. This approach was applied successfully by Ayres et al. (1988). We believe that it would also help in the interpretation of large-scale experiments such as wide plate crack arrest experiments.

Comparison of the COD data obtained with the HEDIT method and with FRASTA indicates good qualitative agreement between the two methods, since both show a significant increase in COD and COA as the position of crack arrest is approached and also a large amount of blunting of the arrested crack tip. Comparison of the data in Tables 1 and 2 shows good quantitative agreement between the two techniques when the COD values at and after arrest are compared for corresponding positions along the crack front (i.e, at the center of the specimen). For the crack extension phase immediately before arrest, the HEDIT measurements seem to overestimate the COD. This overestimate may be due to a component of the displacement associated with plastic deformation of the uncracked specimen ligament before passage of the running crack.

The overall good agreement between HEDIT and FRASTA results gives confidence in the measurement techniques and indicates that reasonable estimates of the COD and the near tip profiles can be obtained from remote dynamic displacement measurements. Therefore, it appears possible to estimate the near tip crack opening profile during crack arrest and reinitiation events by placing a number of dynamic displacement transducers on fracture specimens, provided the crack extension history is also independently measured. This approach may prove useful in crack arrest experiments using small compact crack arrest specimens to obtain direct estimates of the arrest toughness in terms of the COD.

Since FRASTA is a posttest measurement technique, it requires no dynamic instrumentation of dynamic fracture specimens to obtain COD data. Contrary to calculated toughness values, the FRASTA-obtained COD does not require knowledge of the transient boundary conditions and does not rely on two-dimensional field assumptions. As a local measurement, the FRASTA-obtained COD truly reflects the influence of through-the-thickness deformations on the crack tip deformation field. Therefore, comparison of FRASTA-measured COD values and stress intensity factor based toughness values could help explain some differences in arrest behavior observed for similar materials tested at comparable temperatures but using different specimen sizes, geometries, and thicknesses. Indeed, the good correlation between the crack propagation and arrest events and the evolution of the COD and COA observed in our investigation suggests that the COD and COA could be useful parameters for characterizing dynamic fracture in the presence of plasticity and viscoplasticity. This point is addressed in more detail in Kobayashi and Giovanola (1988).

CONCLUSIONS

Measurements of COD and COA during cleavage crack arrest experiments using two independent techniques--one based on global crack face displacement measurements and the other on direct measurements of the crack tip deformation--lead to the following conclusions:

- Crack face opening profiles can be readily measured during dynamic crack propagation experiments and can serve to verify numerical simulations of the experiments.
- Estimates of the COD during dynamic crack propagation and arrest can be obtained from global crack face displacement measurements and from crack extension history information.
- Measurements of the local COD with FRASTA can provide a way to evaluate crack arrest data from different test geometries and to assess the influence of specimen size, specimen thickness, and triaxial constraint on the arrest toughness.

ACKNOWLEDGMENTS

This investigation was supported by the Electric Power Research Institute (EPRI) under Contract RP2455-7, Dr. D. M. Norris and Mr. T. Griesbach, Program Managers. The authors are also indebted to Drs. D. J. Ayres and R. J. Fabi and Messrs. R. Y. Schonenberg and D. A. Peck of Combustion Engineering, Inc., for their collaboration during the HEDIT measurements and for making the fracture surfaces and their experimental results available.

REFERENCES

Ayres, D. J., R. J. Fabi, R. Y. Schonenberg, and D. M. Norris (1988). In: *Fracture Mechanics: Nineteenth Volume, ASTM STP*, in preparation, American Society for Testing and Materials, Philadelphia.

Bryan, R. H., B. R. Bass, J. G. Merkle, C. E. Pugh, G. C. Robinson and G. D. Whitman (1986). The heavy-section steel technology pressurized-thermal-shock experiment, PTSE-1, *Eng. Fract. Mech.*, 23, 81-97.

DeWit, R. and R. J. Fields (1988). In: *Fracture Mechanics: Twenty-First Volume, ASTM STP,* in preparation, American Society for Testing and Materials, Philadelphia.

Giovanola, J. H., T. Kobayashi, R. W. Klopp, T. Gaines, and R. Arwood (1988). A note on dynamic displacement measurements using Hall effect sensors. *Submitted to J. of Test. and Eval.*

Kobayashi, T. and J. H. Giovanola (1988). Crack opening profile observations for dynamic cleavage crack propagation and arrest. *Submitted to J. Mech. Phys. Solids.*

Kobayashi, T. and D. A. Shockey (1987). A fractographic investigation of thermal embrittlement in cast duplex stainless steel, *Met. Trans.*, 18A, 1941-1949.